COMMISSIONING OF THE TAIWAN PHOTON SOURCE

C. C. Kuo, J. Y. Chen, M. S. Chiu, P. J. Chou, Y. C. Liu, H. J. Tsai,
F. H. Tseng, K. T. Hsu, G. H. Luo and C. T. Chen
National Synchrotron Radiation Research Center, Hsinchu 30076, Taiwan

Abstract

The Taiwan Photon Source (TPS) is a 3-GeV third-generation synchrotron light source located in Hsinchu, Taiwan. After ground breaking on February 7, 2010 and five years of construction and hardware developments, commissioning of the beam began on December 12, 2014. The booster ring reached the design energy of 3 GeV on December 16. Beam transferred to the storage ring and first accumulation at 3 GeV produced the first synchrotron light on December 31. This report presents results and experience of the TPS commissioning.

INTRODUCTION

The 3-GeV TPS is located on the campus of NSRRC in Hsinchu Science Park together with the 1.5-GeV Taiwan Light Source (TLS) which has been in operation since 1993. To expand the capacity for research with synchrotron light and its capability at NSRRC, we initiated in 2004 a feasibility study for the construction of a medium energy and low emittance light source. Funding of the TPS project was approved in 2007 and a ground-breaking ceremony of TPS was held on February 7, 2010. The civil construction required about four years to complete. The installation of TPS accelerator components began in October 2013 when beneficial occupancy was available. Most installation work for the Linac and booster ring was completed by the end of July 2014. Permission for commissioning the TPS with beam was issued by the AEC on August 1. Tests of the system and improvements of the harware with beam have proceeded since then.

The 150-MeV beam from the Linac to the booster was available in mid August and tests of the booster power supplies conducted in parallel. Hardware optimizations were in progress like reducing the post-pulse residual field in the booster injection kicker or repair of a burned booster-dipole power supply due to overheating of the ground-current protection circuit-board during a full power ramping test.

At the beginning of September, a multi-turn circulating beam was observed in the booster ring. The beam survived up to 35 ms in mid September, but capture and storage of the beam did not succeed with the RF turned on. Attempts to correct orbit distortions within 4 mm still failed to capture beam. We found also that the corrector strengths required to get many turns were three times the simulated values. The beam pipes of the booster ring, made of stainless steel 304, have an elliptical shape, 35 mm (H) and 20 mm (V), and thickness of 0.7 mm.

Distortion and misalignment of the pipes could be critical. Care was taken to realign the chambers and magnet positions. On November 12 it was recognized that the relative permeabilty (ranging from 1.2 to 2.0) of the pipes arising from the cold-drawn process of the pipe manufacture was too large. The magnetic fields of the combined-function dipoles (including quadrupole and sextupole gradients in dipole magnets) at 150 MeV could generate errors an order magnitude higher than tolerances. These chambers were taken apart and heat treated up to 1050 °C and then reinstalled within three weeks [1]. The relative permeability of the pipes after heat treatment was reduced to less than 1.01 [2].

Soon the beam survived 50 ms on December 11 and a beam was stored on December 12. Tests of the energy ramping began on December 15 and 3 GeV were reached the next day.

To prepare the extraction from the booster ring and its injection into the storage ring TPS was shut down from December 19 to 23. During this period, installation work and subsystem tests of the booster to storage ring transfer line (BTS) as well as the storage ring continued. The DC extraction septum operating at 3 GeV severely affected the booster capture at 150 MeV and ramping efficiency because of residual leakage field from the shielded septum chamber. Without further effort to shield the leakage field, we extracted a 1.5-GeV beam instead and injected it into the storage ring on December 26; the beam was stored the next day. After adding extra correctors nearby the DC extraction septum, extraction at 3 GeV became feasible on December 30 and an accumulated beam of up to 5 mA could be stored on December 31, 2014. The DC septum was replaced with an AC type in January, 2015.

Two 5-cell PETRA cavities were used to commission the storage ring in Phase I. The maximum stored current of 100 mA was achieved on March 26 after improvement of the RF feedback loop. Cleaning with synchrotron light (an accumulated beam dose up to 35 A.h before shutdown in April) could effectively improve the vacuum conditions for the commissioning in Phase II with superconducting RF (SRF) cavity modules.

During the commissioning period, the rules for radiation safety were strictly adhered to. In user mode the integrated dose should be less than 2 μSv per 4 h.

Before shutdown for the installation of the SRF and insertion devices (IDs) beginning in April, the hardware improvements, lattice characterization and system optimization etc. proceeded. Diagnostic and control systems played a major role during the commissioning stage [3,4,5]. We adopted middle-layer, high-level

application programs (based on MATLAB), such as Linear Optics with Closed Orbit (LOCO) and Beam-based Alignment (BBA) developed in SSRL-ALS to characterize and to optimize machine functions [6, 7]. Table 1 lists the major design parameters of TPS [8, 9] followed by commissioning results.

Table 1: Major Design Parameters of the TPS Accelerators

storage ring	
circumference /m	518.4
energy /GeV	3.0
Lattice	24-DBA
horizontal emittance /nm rad	1.6
vertical emittance /nm rad	0.016
average beam current /mA	500
momentum compaction (α_1/ α_2)	$2.4\ 10^{-4}/2.1\ 10^{-3}$
betatron tune (ν_x/ν_y)	26.18/13.28
natural chromaticity (ξ_x/ξ_y)	-75 / -26
RF frequency /MHz	499.654
synchrotron booster	
circumference /m	496.8
energy /GeV	0.15~3.0
Lattice	6-MBA
horizontal emittance at 3 GeV /nm rad	10.3
betatron tune (ν_x/ν_y)	14.380/9.302
repetition rate /Hz	3
RF frequency /MHz	499.654
Linac	
energy /MeV	150
charge /nC (MB/SB)	5/1.5
Normalized emittance (π μm rad, H/V)	50/50

LINAC

The performance of the linear accelerator (Linac, 150 MeV, Research Instruments Ltd) was accepted at the NSRRC test site in 2011. The components were later transferred to the TPS site between March and June 2014. Tests with beam began in August. Along with Linac re-commissioning, the Linac to Booster (LTB) transfer line was tested. The beam properties of the Linac such as charge intensity, bunch train, energy, energy spread, energy jitter etc. were re-measured. The beam size, transmission rate etc. in the LTB were also measured and lattice functions were adjusted to increase transmission as well as beam capture in the booster ring [10].

BOOSTER RING

The TPS booster ring shares the tunnel with the storage ring. To optimize the number of magnets, combined-function dipole and quadrupole magnets were adopted. Dipole magnets include defocusing quadrupole and defocusing sextupole fields. One combined-function focusing quadrupole family with focusing sextupole field and three separated-function quadrupole families are used for optics matching and two sextupole families are for chromaticity adjustment. The sizes of magnets and vacuum chambers were minimized to save space, construction cost and power consumption.

After reducing the permeability of the pipes, we had

quickly a stored and ramped beam. Figure 1 shows the stored beam with active RF. The 150-MeV injected beam could be ramped up to 3 GeV and then ramped down to 1.3 GeV with sinusoidal ramping and modified tracking waveforms in power supplies for dipole and quadrupole magnets. The overall transmission efficiency of the beam intensity in the booster was about 60 % during capture and ramping, as illustrated in Fig. 2. Independent sextupoles of two families were ramped with sinusoidal waveforms to get desired chromaticities and all were powered as defocusing sextupoles that might be due to insufficient sextupole components in the combined-function dipole magnets. Tune variations were kept within 0.1 as shown in Fig. 3. There was no ramping of correctors while the orbit excursions during energy ramping was kept to 3 mm in the horizontal and 1 mm in the vertical plane. Lattice functions were measured by turn-by-turn BPM data, which agreed satisfactorily with the model. A detailed report is given in these proceedings [11].
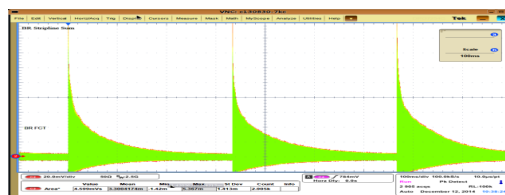

Figure 1: Stored beam in the TPS booster ring at 150 MeV on 2014 December 12.
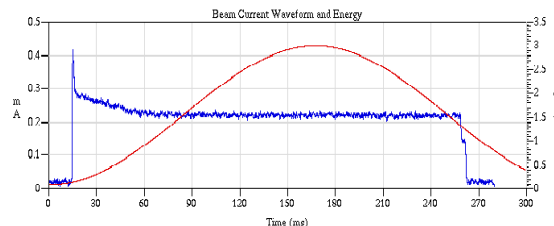

Figure 2: Beam current (blue, left scale) of the TPS booster ring during ramping. The total efficiency of transmission is about 60 % for extraction at 3 GeV. Energy in red (right scale).
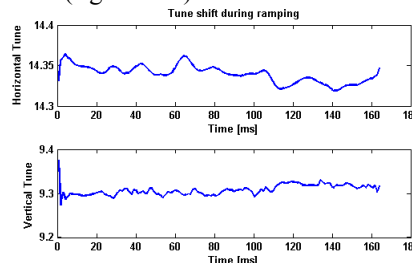

Figure 3: Betatron tune tracking during ramping in the TPS booster ring. Tune changes are within 0.1.

STORAGE RING

Although the DC extraction septum affected the booster beam at the 3-GeV settings, beam extraction at 1.5 GeV was possible. The extraction at 1.5 GeV showed that the beam behaved as designed in the BTS. We injected a 1.5-GeV beam into the storage ring and obtained multiple turns with one horizontal corrector only. A stored and accumulated beam was obtained with the adjustment of

2: Photon Sources and Electron Accelerators

A05 - Synchrotron Radiation Facilities

RF, quadrupole and sextupole magnets and kickers. The stored beam at 1.5 GeV is shown in Fig. 4.

When 3.0-GeV injection was realized after adding extra correctors nearby the DC extraction septum, storage and accumulation of the beam proceeded smoothly, even without any corrector. We accumulated and stored a beam of 5 mA on December 31, 2014 as shown in Fig. 5.
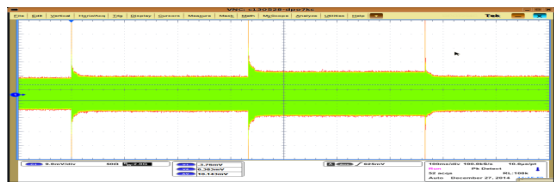

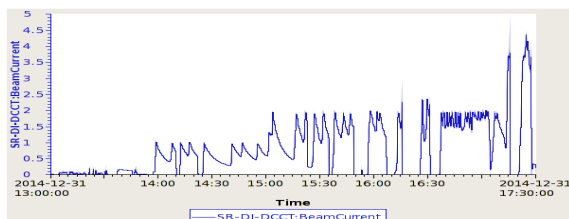Figure 4: Stored beam at 1.5 GeV in TPS storage ring.

Figure 5: Stored and accumulated beam at 3.0 GeV in the TPS storage ring on December 31, 2014.

Closed Orbit

Closed orbit distortions (CODs) were measured after beam storage. Using 166 BPM and 168 correctors in each plane, CODs were corrected to less than 3 mm horizontal and 1 mm vertical. The machine orbit response was found to be inconsistent with the model in the horizontal plane. The quadrupole model required modification. We decided to correct the lattice with LOCO and also to perform BBA to obtain the BPM offsets with respect to the field center of the nearby quadrupole magnets. Each BBA measurement required 5 h. Figure 6 shows the BBA results on March 3, 2015.
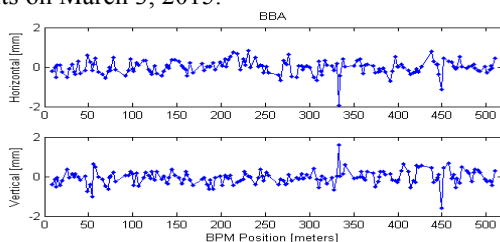

Figure 6: BPM-quadrupole center offset. H_{rms}=0.344 mm, V_{rms}=0.346 mm.

The LOCO results revealed a few BPM discrepancies that were thus corrected. After three iterations of LOCO runs and BBA, the measured orbit without correctors was 1.78 mm rms horizontal and 1.04 mm rms vertical, as shown in Fig. 7. The *bare* COD results demonstrate the excellent work on alignment and magnets [2, 12]. After orbit correction, the CODs were reduced to 103 μm rms horizontal and 69 μm rms vertical (Fig. 8). Employing less than 20 eigenvalues, moderate corrector strengths of less than 0.25 mrad (0.038 mrad rms) horizontal and 0.1

mrad (0.018 mrad rms) vertical were used. With more eigenvalues and stronger corrector strengths the residual orbit can be decreased further.
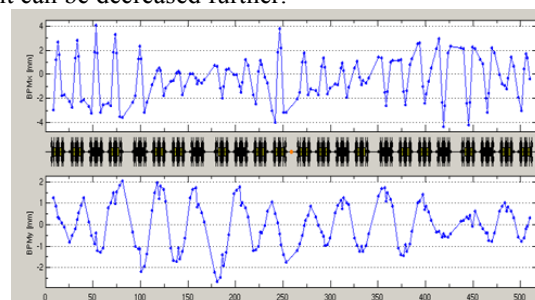

Figure 7: Closed orbit distortions without correctors in the TPS storage ring after three LOCO iterations and BBA.
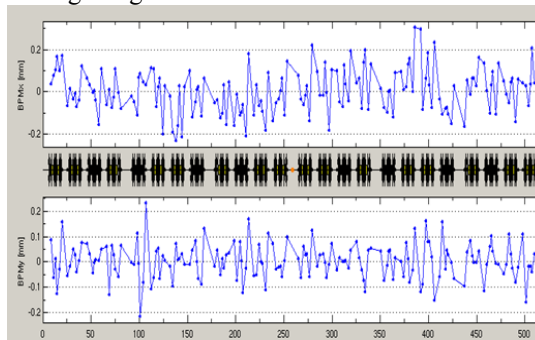

Figure 8: Closed orbit distortions after correction and beam-based alignment of the TPS storage ring.

Linear Optics and Coupling Correction

LOCO was the major application program for optical calibration and optimization. The deviations in the beta function were reduced from 8.91 to 1.44 % rms horizontal and from 10.94 to 0.68 % rms vertical after three iterations of corrections. Figure 9 shows the beta beating in both planes. The horizontal dispersion function agreed satisfactorily with the model following LOCO runs; the spurious vertical dispersion was 2.43 mm rms. Figure 10 shows variations of the quadrupole strength deviating from hard-edge model settings. These variations might be due to transfer function of magnetic field, fringe field, sextupole feed-down and power supplies, etc. The BPM gain and roll as well as the corrector gain and tilt were also fitted and corrected. The achromat lattice configurations were measured and calibrated accordingly.
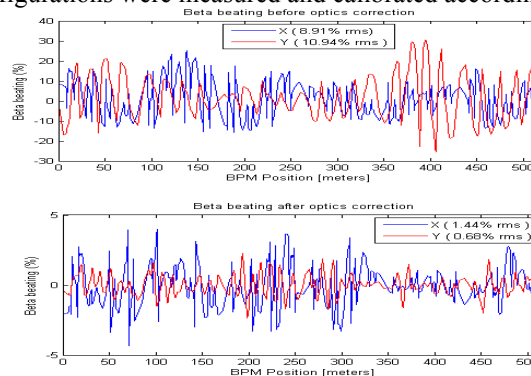

Figure 9: Beta beating before (above) and after three iterations (below) of LOCO (note difference of scale).
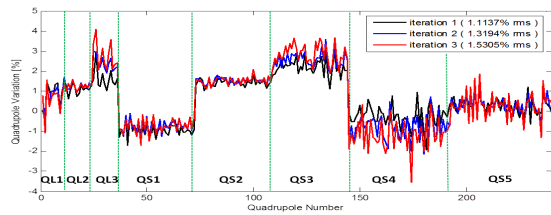
Figure 10: Variations of the fitted quadrupole strength with respect to hard-edge model values after LOCO.

The linear coupling was corrected in the LOCO runs. We used 168 skew quadrupoles to correct the betatron coupling and the vertical dispersion. The closest tune gaps were 0.0005 and 0.0065 with and without skew quadrupole magnets, respectively, as illustrated in Fig. 11. The vertical dispersion was reduced to 1.77 mm rms with skew quadrupole corrections. Table 2 lists the emittance ratios contributed from the betatron coupling for working tune of $\nu_x=26.1831$ and $\nu_y=13.2945$. The vertical dispersion contributions are estimated and measured values from a pinhole camera are shown as well.
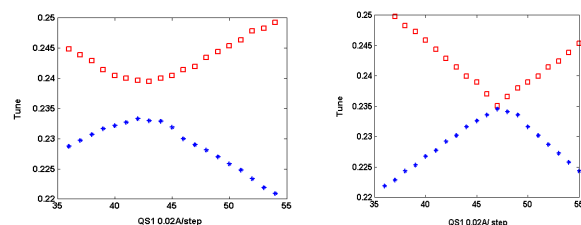

Figure 11: Minimal tune gap before (left) and after (right) correction of betatron coupling with skew quadrupole magnets.

Table 2: Emittance Coupling Ratio of TPS

emittance ratio	w/o skew quad	w/ skew quad
betatron coupling	0.170 %	0.001 %
vertical dispersion	0.156 %	0.038 %
pinhole camera	1.65 %	0.96 %

The uncertainty in the pinhole camera measurements was due mainly to the beam orbit noise and instabilities, and the system resolution. The measurements were conducted at low stored beam current with a brief integration and assuming a natural energy spread. Table 3 lists the measured emittance from the pinhole camera [3].

Table 3: Measured Emittance of TPS with Pinhole Camera

Emittance	w/o skew quad	w/ skew quad
Horizontal /nm rad	1.55	1.64
Vertical /nm rad	0.0256	0.0157

Nonlinear Chromaticity

The RF frequency centering was corrected with a dispersion fit and also on measuring the crossing in the tune shift with energy at various chromaticity settings. The measured center RF frequency differed from the nominal value by +1.228 kHz indicating that the ring

circumference was smaller by 1.27 mm. The natural chromaticities were measured on varying the dipole field strength. The dipole field was well calibrated. The measured natural chromaticities (horizontal/vertical) were -72.5/-25.8, which are very close to the model values -75/-26.

Using an eight-family sextupole scheme, nonlinear beam dynamics were optimized and natural chromaticities were corrected to be slightly positive. Tune shift as a function of energy was measured by varying the RF frequency. Because of the small first-order momentum compaction factor, the second order must be taken into account in the relation between energy and RF. Figure 12 shows that the measured acceptance of the lattice energy is in good agreement with the model simulation.
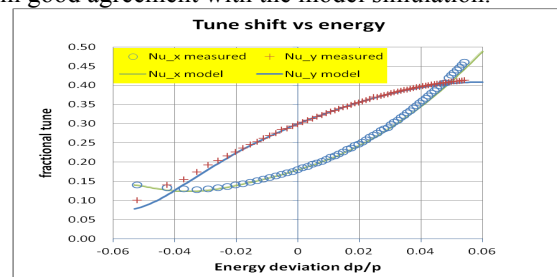

Figure 12: Tune shift vs energy of TPS storage ring with chromaticity 2.5/3.4 in horizontal/vertical planes.

Beam Filling

The beam in the storage ring can be filled in a multi-bunch mode for fast injection or a single-bunch mode to control the filling pattern and during top-up opertion. The total efficiency of beam injection from the booster to the storage ring was 80 % and an accumulation rate of ~0.4 mA/s in multi-bunch injection was obtained. The single-bunch impurity was near 10^{-5} due to an rf knock-out technique. Figure 13 shows the single-bunch intensity measured with time-correlated single photon counting (TCSPC).
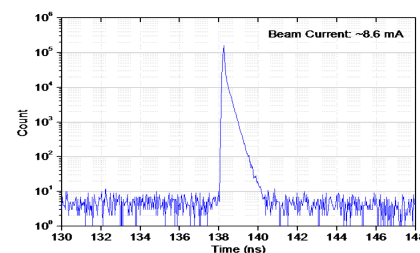

Figure 13: Single-bunch intensity with TCSPC. Impurity is near 10^{-5}.

Impedance and Instability

A dual-sweep streak camera (C10910 Hamamatsu Photonics) was used to measure the longitudinal motion of the beam and the bunch length. The bunch length (rms) as a function of bunch current with RF at 2.4 MV is shown in Fig. 14. Fitting with Zotter's potential-well distortion cubic equation, we obtained a longitudinal broadband impedance of $|Z/n|$=0.12 Ω [13]. The tune

variation as a function of bunch current was -0.0005/mA in the horizontal and -0.0012/mA in the vertical plane, respectively. The effective transverse impedance was thus 0.154 MΩ/m horizontal and 0.175 MΩ/m vertical. The results indicate a smooth vacuum chamber.
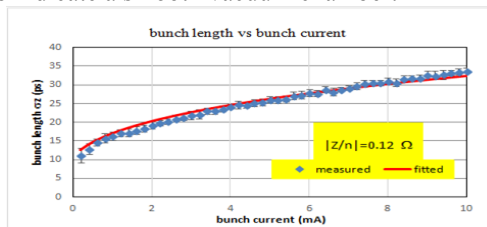

Figure 14: Bunch length as a function of bunch current for RF=2.4 MV. Fitted longitudinal broadband impedance is $|Z/n| = 0.12$ Ω.

Running with PETRA cavities, to suppress the vertical instability in single-bunch operation a large chromaticity was required. The record bunch current was 12 mA, limited by heating in the RF windows. The beam current might reach more than 100 mA in multi-bunch operation with two PETRA cavities. We observed a strong synchrotron dipole motion and obtained less than 50 mA before we found that the bandwidth in the RF feedback loop was too large such that a synchrotron sideband entered the loop. After narrowing the bandwidth and increasing the chromaticity to 2.4 and 3.5 in the horizontal and vertical plane, respectively, 100 mA became practicable, but transverse instabilities were observed, which were damped with a bunch by bunch feedback damper. A new threshold for the longitudinal instability appeared again at ~80 mA. We expect that this instability will weaken after vacuum improvement and replacement of the 5-cell PETRA cavities with SRF.

Orbit Stability

During the stages of design and construction stringent criteria for orbit stability in the sub-μm range were applied. From the BPM noise spectrum we found that noise at 29 Hz was the dominant source, which might be due to vibrations of chambers and girders as induced by mechanical and turbo pumps [14]. After pumps were turned off, the noise level was much decreased. The water turbulence in vacuum chambers is another source of noise. Figure 15 shows the integrated noise level in each plane. Efforts to eliminate other sources of noise will be undertaken in the near future.
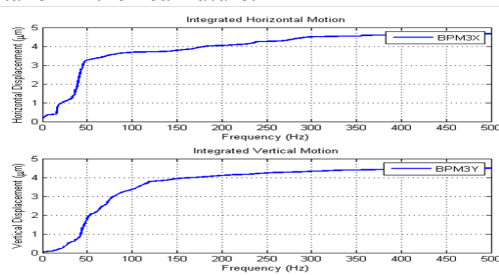

Figure 15: Integrated orbit and BPM noise level in each plane.

Vacuum and Lifetime

Vacuum chambers are made of Al alloy. The static pressure before beam commissioning was 2.8 10^{-8} Pa and reached 2.37 10^{-8} Pa after 35 A.h beam dose. The dynamic pressure was 1.17 10^{-7} Pa/100 mA and the lifetime at 100 mA reached more than 6 hours [15].

FUTURE PLAN

The commissioning of SRF and ten IDs is scheduled to begin in September 2015 and beamline commissioning will proceed thereafter. Much challenging work lies ahead but we shall succeed. Operation for users are scheduled to begin in mid 2016.

ACKNOWLEDGEMENT

REFERENCES

[1] I. C. Sheng, et al., "Demagnetized Booster Chambers in TPS", these proceedings.

[2] J. C. Jan, et al., "Magnet Design and Control of Field Quality for TPS Booster and Storage Ring", these proceedings.

[3] C. Y. Liao, et al., "Preliminary Beam Test of Synchrotron Radiation Monitoring System at Taiwan Photon Source", these proceedings.

[4] P. C. Chiu, et al., "Commissioning of BPM System for TPS Booster Synchrotron", these proceedings.

[5] Y. S. Cheng, et al., "Control System Software Environment and Integration for the TPS", Proc. PCaPAC2014, Karlsruhe, Germany, 2014.

[6] G. Portmann, et al., "An Accelerator Control Middle Layer Using MATLAB", Proc. PAC. 2005, p.4009.

[7] J. Safranek, "Experimental Determination of Storage Ring Optics Using Orbit Response Measurement", *Nucl. Inst. and Meth*. **A388**, 27 (1997).

[8] C. C. Kuo, et al., "Progress Report of TPS Lattice Design", Proc. PAC. 2009, p.2273.

[9] C. C. Kuo, et al., "Accelerator Physics Issues for TPS", Proc. IPAC. 2010, p.36.

[10] H. P. Chang, et al., "TPS Linac Relocation and Beam Test of the LTB Transfer Line", these proceedings.

[11] H. J. Tsai, et al., "Hardware Improvements and Beam Commissioning of the Booster Ring in Taiwan Photon Source", these proceedings.

[12] T. C. Tseng, et al, "The Auto-Alignment Girder System of TPS Storage Ring", these proceedings.

[13] B. Zotter, in "Handbook of Accelerator Physics and Engineering", edited by A. Chao and M. Tigner, World Scientific, 2013, p146, 2nd edition.

[14] C. H. Huang, et al., "Vibration Measurement of the Magnets in the Storage Ring of TPS", these proceedings.

[15] I. C. Yang, et al., "Behaviour of Vacuum Pressure in TPS Vacuum System ", these proceedings.